Journal of Fluorine Chemistry 144 (2012) 182–188

Contents lists available at SciVerse ScienceDirect

Journal of Fluorine Chemistry

journal homepage: www.elsevier.com/locate/fluor

The nonisothermal crystallization kinetics of surface fluorinated polypropylene/polypropylene blend

Weihong Guo [a], Lei Gao [a], Guanlong Chen [a], Yan Zhang [a], Haoming He [c,**], Tian Xie [c], Sanke Yang [c], Shimin Ding [a], Xianjin Yang [a,b,c,*]

[a] Key Laboratory for Advanced Materials and Institute of Fine Chemicals, East China University of Science and Technology, 130 Meilong Road, Shanghai 200237, China
[b] Key Laboratory of Organofluorine Chemistry, Shanghai Institute of Organic Chemistry, Chinese Academy of Sciences, 345 Lingling Road, Shanghai 200032, China
[c] Wengfu Group Co. Ltd., Guizhou 550000, China

ARTICLE INFO

Article history:
Received 25 August 2012
Received in revised form 28 September 2012
Accepted 28 September 2012
Available online 8 October 2012

Keywords:
Surface fluorination
Polypropylene
Blend
Crystallization kinetics
Macrokinetic model

ABSTRACT

The surface fluorinated polypropylene/polypropylene blend (SFPP/PP) was obtained by direct fluorination of polypropylene particle with 3% F_2/N_2 gas and subsequently blending it with polypropylene particle and antioxidant 1010. The nonisothermal crystallization kinetics properties of SFPP/PP were investigated using differential scanning calorimetry and the results indicated the compatibility of SFPP/PP is good, the crystallization temperature T_0, T_c and crystallization activation energy ΔE are increased, whereas enthalpy ΔH_c are decreased with the incorporation of fluorine to PP. Several macrokinetic models such as Jeziorny, Ozawa and Mo are used to analyze the nonisothermal crystallization behavior of the blend, among which Mo equation supplies a convenient and reasonable kinetic approach to describe its crystallization process.

1. Introduction

Fluorine is unique in that it is possible to replace hydrogen by fluorine either singly or multiply in an organic or material molecule, and in so-doing creates a potentially infinite extension to organic or material chemistry that is entirely synthetic, and the introduction of fluorine into organic or material molecule usually endows it with novel properties, which is broadly applied in pharmaceutics, insecticide and material fields [1]. Fluorine-containing polymer can be prepared by the polymerization of fluoromonomer or the direct fluorination of polymer. Surface fluorination of polymer with elemental fluorine is one of important direct fluorination strategies because it supplies a low-cost and simple-operation method to obtain fluorine-containing polymers with some unique properties [2]. However, surface fluorination can only modify the surface properties for fluorine atoms scarcely entering the inner layer of a polymer (usual fluorinating depth does not exceed several μm) [3]. Blending a polymer with its corresponding fluoropolymer supplies a seemingly reasonable method to acquire a homogenous fluorine-containing composite, whereas compatibility remains a big problem.

We envisage that the simply blending of a polymer with its corresponding surface fluorinated polymer possibly makes a convenient and inexpensive way for preparing a homogenous fluorine-containing blend, which has a possibility to display some unique properties, albeit the fluorine content in the composite is low. Herein, we prepare the internally fluorine-containing polypropylene blend by the surface fluorination of polypropylene particle and subsequently alloying it with polypropylene particle and antioxidant 1010. And on the basis of this work, the nonisothermal crystallization kinetics properties of the blend are investigated in order to understand its crystallization behaviors.

2. Results and discussion

2.1. Nonisothermal crystallization behavior of SFPP/PP blend

We begin our studies from the fluorinaton of PP particles (T30, radius 2 mm) with 3% F_2/N_2 mixing gas at room temperature. The EDS analysis shows the surface fluorine content of the fluorinated polypropylene particle (SFPP) is 9.36 at%. And after that, the SFPP particle was mixed with PP particle and some antioxidant 1010 according to the ratio shown in Table 1.

* Corresponding author at: Key Laboratory for Advanced Materials and Institute of Fine Chemicals, East China University of Science and Technology, 130 Meilong Road, Shanghai 200237, China.
** Corresponding author.
E-mail addresses: hehaoming@wengfu.com (H. He), yxj@ecust.edu.cn (X. Yang).

0022-1139/$ – see front matter © 2012 Elsevier B.V. All rights reserved.
http://dx.doi.org/10.1016/j.jfluchem.2012.09.011

Table 1
The raw material composition for SFPP/PP blend.

Sample no.	1	2	3
PP (phr)	100	50	0
SFPP (phr)	0	50	100
Antioxidant 1010 (phr)	1.5	1.5	1.5

Table 2
T_0, T_c, S_i and ΔH_c for all the samples at 7.5 °C/min cooling rate.

Sample no.	T_0 (°C)	T_c (°C)	S_i	ΔH_c (J/g)	$t_{1/2}$ (min)
1	119.2	113.1	0.437	124.1	0.655
2	121.9	116.1	0.360	116.9	0.723
3	124.6	118.4	0.339	106.4	0.796

Furthermore, the above mixtures **1**, **2** and **3** were blended with heating from room temperature to 200 °C and back to room temperature. The DSC exotherms of blends **1**, **2** and **3** recorded during cooling cycles at 7.5 °C/min cooling rate are depicted in Fig. 1.

From Fig. 1, some useful DSC crystallization parameters [4] such as onset (T_0), peak crystallization temperatures (T_c), the nucleation rate (S_i) [5] and crystallization enthalpy (ΔH_c) corresponding to 7.5 °C/min cooling rate for all the samples **1**, **2** and **3** are obtained and listed in Table 2.

The crystallization process of polymer includes a nuclei formation process and a spherulite growth process. A distinctly increasing values of onset crystallization temperature T_0 and peak crystallization temperature T_c in samples **2** and **3** by comparison with that in sample **1** (columns 2 and 3 in Table 2) demonstrate fluorination led to an earlier crystallization occurrence in the cooling nonisothermal crystallization process. The lower S_i value for samples **2** and **3** than **1** (column 4 in Table 2) means that the introduction of C–F bonds into the inner layer of a composite may decrease its nucleation rate. While the smaller ΔH_c value and bigger $t_{1/2}$ for samples **2** and **3** than that for sample **1** (column 5 in Table 2) indicate the incorporation of fluorine decreases its absolute value of crystallinity and overall crystallization rate, possibly owing to that the fluorinated polypropylene molecule chain is difficult to enter the crystal lattice.

Then, for these blends, the investigation of crystallization process at different nonisothermal cooling crystallization rates is carried out. Fig. 2 represents the DSC cooling curve for composites **1**, **2** and **3** at 2.5, 5, 7.5 and 10 °C/min cooling rates, from which, T_c, T_0 and $t_{1/2}$ values are recorded and listed in Table 2.

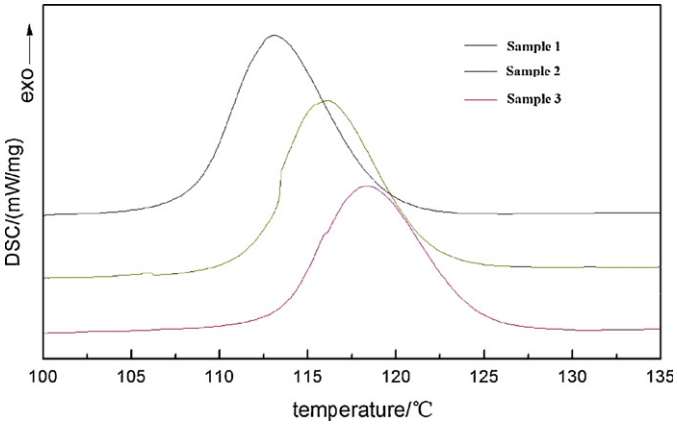

Fig. 1. Heat flow versus temperature in the nonisothermal crystallization for blends **1**, **2** and **3** at 7.5 °C/min cooling rate.

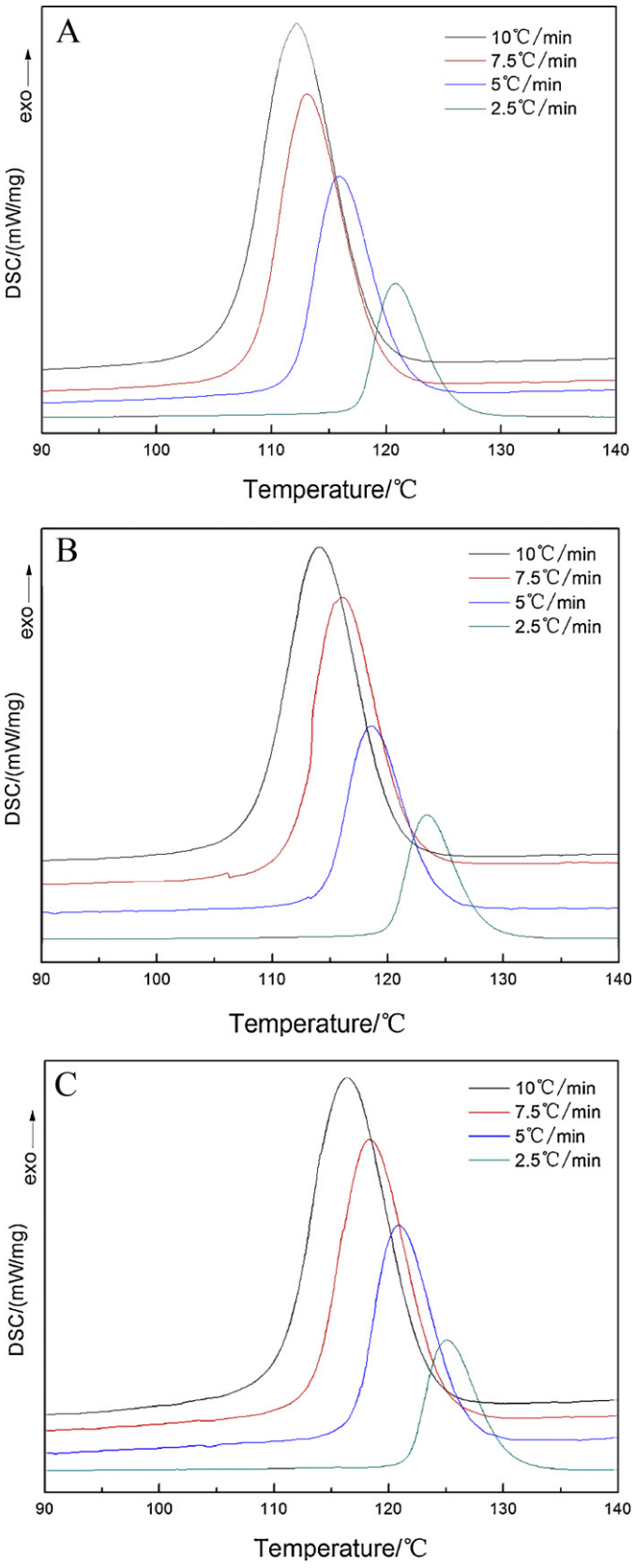

Fig. 2. The DSC curves for samples **1**, **2** and **3** at different cooling crystallization rates: (A) Sample **1**, (B) Sample **2**, and (C) Sample **3**.

Table 3
The DSC data for samples **1**, **2** and **3** at different cooling crystallization rates.

Sample no.	R (°C/min)	T_0 (°C)	T_c (°C)	$t_{1/2}$ (min)
1	2.5	125.7	120.8	1.813
	5	121.6	115.9	1.058
	7.5	119.2	113.1	0.655
	10	118.7	112.1	0.630
2	2.5	128.2	123.4	1.788
	5	124.0	118.6	1.017
	7.5	121.9	116.1	0.721
	10	120.4	114.1	0.610
3	2.5	130.2	125.1	1.728
	5	126.5	120.8	1.041
	7.5	124.6	118.4	0.795
	10	123.1	116.3	0.646

From Fig. 2, with the increase of cooling rate, crystallization peak broadening and left shifting are apparently observed for all the samples. And the data listed in Table 3 indicate that, for different samples at the same cooling rate, T_0 and T_c for samples **2** and **3** are higher than that for sample **1** (columns 3 and 4 in Table 3). For the same sample at different cooling rates, $t_{1/2}$ values reduce with the rise of cooling rate (column 5 in Table 3), while for different samples at same cooling rate, $t_{1/2}$ values are close without consistent changing tendency (column 5 in Table 3). For example, at 2.5 °C/min cooling rate, the $t_{1/2}$ values change as follows: $t_{1/2\text{-sample 1}} > t_{1/2\text{-sample 2}} > t_{1/2\text{-sample 3}}$, which can be presumed that, under this condition, the addition of SFPP slightly enhances the nucleation ability of polypropylene. While at 7.5 °C/min cooling rate, the $t_{1/2}$ values change as follows: $t_{1/2\text{-sample 1}} < t_{1/2\text{-sample 2}} < t_{1/2\text{-sample 3}}$, which probably is mainly due to the SFPP hindering the PP crystal growth.

Furthermore, the relative crystallinity X was calculated according to Eq. (1):

$$X = \frac{\int_{T_0}^{T} (dH_c/dT)dT}{\int_{T_0}^{T_\infty} (dH_c/dT)dT} \quad (1)$$

where T_0 and T_∞ is the initial and terminal crystallization temperature, respectively. And dH_c represents the change of exothermal enthalpy for the crystallization at dT temperature range. In Fig. 2, the temperature can be substituted by time t according to Eq. (2):

$$t = \frac{T - T_0}{R} \quad (2)$$

where T is the crystallization temperature at time t, T_0 is the onset crystallization temperature, and R is the cooling rate. Then the relationship of relative crystallinity X versus crystallization time t at various cooling rates during nonisothermal crystallization can be described as shown in Fig. 3.

2.2. Nonisothermal crystallization kinetics analysis

On the basis of the above experiments, the nonisothermal crystallization kinetics analysis is carried out using Jeziorny, Ozawa and Mo models [6].

2.2.1. Jeziorny analysis

The crystallization kinetics is often interpreted with the aid of well-known Avrami model [7]. Usually, Avrami equation for the isothermal crystallization kinetics process of a polymer is described as follows:

$$X = 1 - \exp[-K(t - t_0)^n] \quad (3)$$

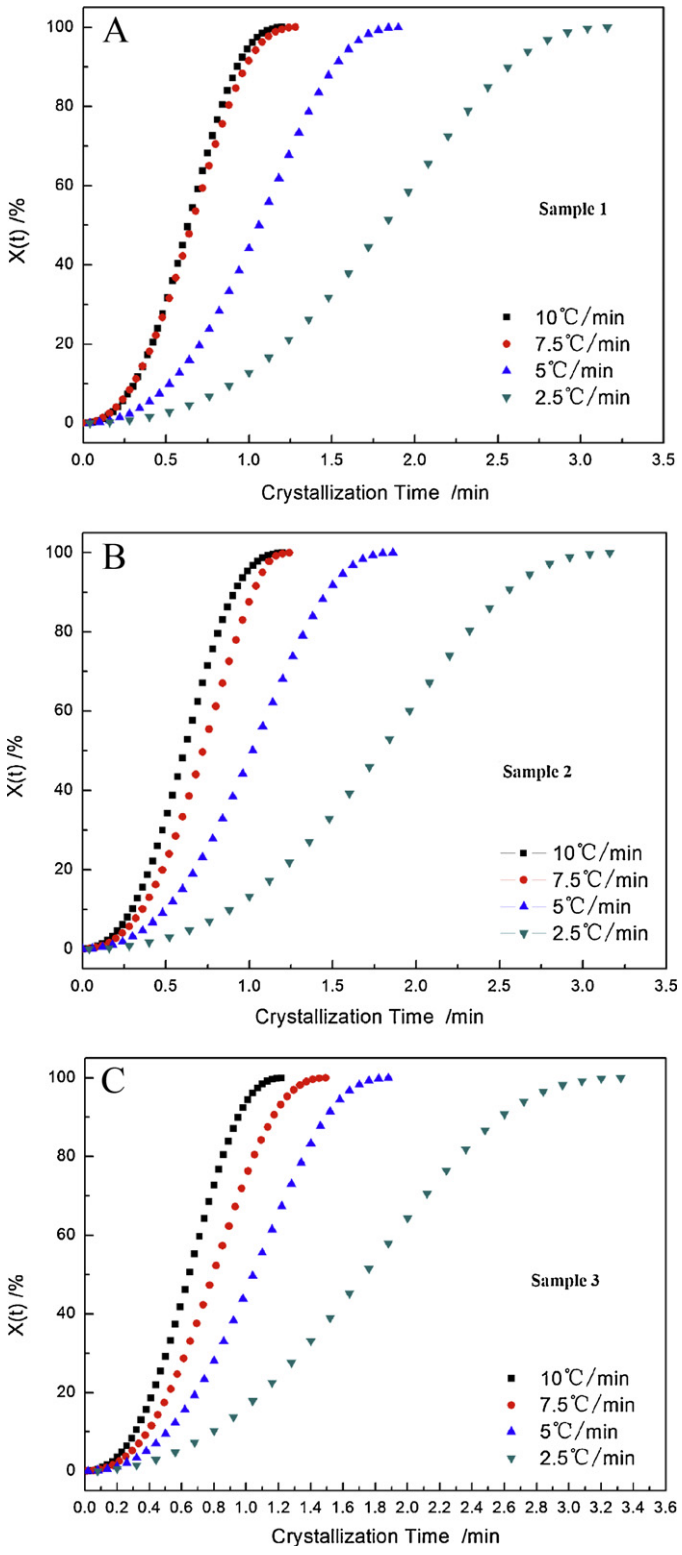

Fig. 3. The plot of relative crystallinity X versus crystallization time t at different cooling rates: (A) Sample **1**, (B) Sample **2**, and (C) Sample **3**.

At constant temperature T, X stands for the relative crystallinity between the crystallization time t and t_0, K is the crystallization rate constant involving both nucleation and spherulite growth; n is Avrami exponent, depending on the nature of nucleation and growth geometry of crystals.

In order to simplify the aforementioned equation, it is often expressed in the double logarithmic linear form as given in Eq. (4):

$$\log[-\ln(1-X)] = \log K + n \log t \quad (4)$$

Jeziorny [8] pointed out that the value of the rate constant, K, should be corrected for the rate of crystallization depends on the cooling rate employed. Considering the influence of various cooling rates on the nonisothermal crystallization condition, Jeziorny gave the final form of the parameter characterizing the kinetics during nonisothermal crystallization as Eq. (5):

$$\log K_c = \log K / R \quad (5)$$

where K is the crystallization rate constant and K_c is the modified crystallization rate constant with respect to cooling rate R.

Plotting $\log[-\ln(1-X)]$ against $\log t$ for all the composites **1**, **2** and **3** at various cooling rates, the results are exhibited in Fig. 4. Observation shows that the plot consists of two straight lines with a gentle deviation in the second stage from the first one. Usually, this deviation is considered to be due to the secondary crystallization caused by the spherulite impingement in the later stage. The linear portions are almost parallel to each other at various cooling rates and left shift with the increase of R, indicating that the nucleation mechanism and crystal growth geometries are similar for the first and secondary crystallization at all cooling rates.

Both K and n are the parameters used to qualitatively interpret the crystalline morphology and type of nucleation for a particular crystallization condition. Calculated from the intercept and slope of these plots, several parameters, crystallization rate constant K, corrected crystallization rate constant K_c, Avrami component in the first stage n_1 and that in the second stage n_2 are obtained (Table 4). Data observed from Table 4 indicates that, in most cases, at the same cooling rate K and K_c values for samples **2** and **3** are slightly smaller than that for sample **1**, which indicates the crystallization rate usually decreases slightly with the addition of SFPP. Meanwhile, much bigger n_2 than n_1 is observed for all the composites, which might be ascribed to spherulite growth change from two-dimension model in the first stage to three-dimension model in the second stage.

2.2.2. Ozawa analysis

Ozawa [9] extended the isothermal crystallization kinetics theory to the nonisothermal case by assuming that the non-isothermal crystallization procedure comprises of infinitesimally small isothermal crystallization steps or pseudo-isothermal processes. The Ozawa equation is a modification of the Avrami equation, which considers the effect of cooling rate on crystallization from the melt and replaces the crystallization time under isothermal conditions with cooling rate R as follows:

$$X = 1 - \exp[-K(T)/R^m] \quad (6)$$

where $K(T)$ is the Ozawa crystallization rate constant, R is the cooling rate, X is the relative crystallinity at temperature T, and m is

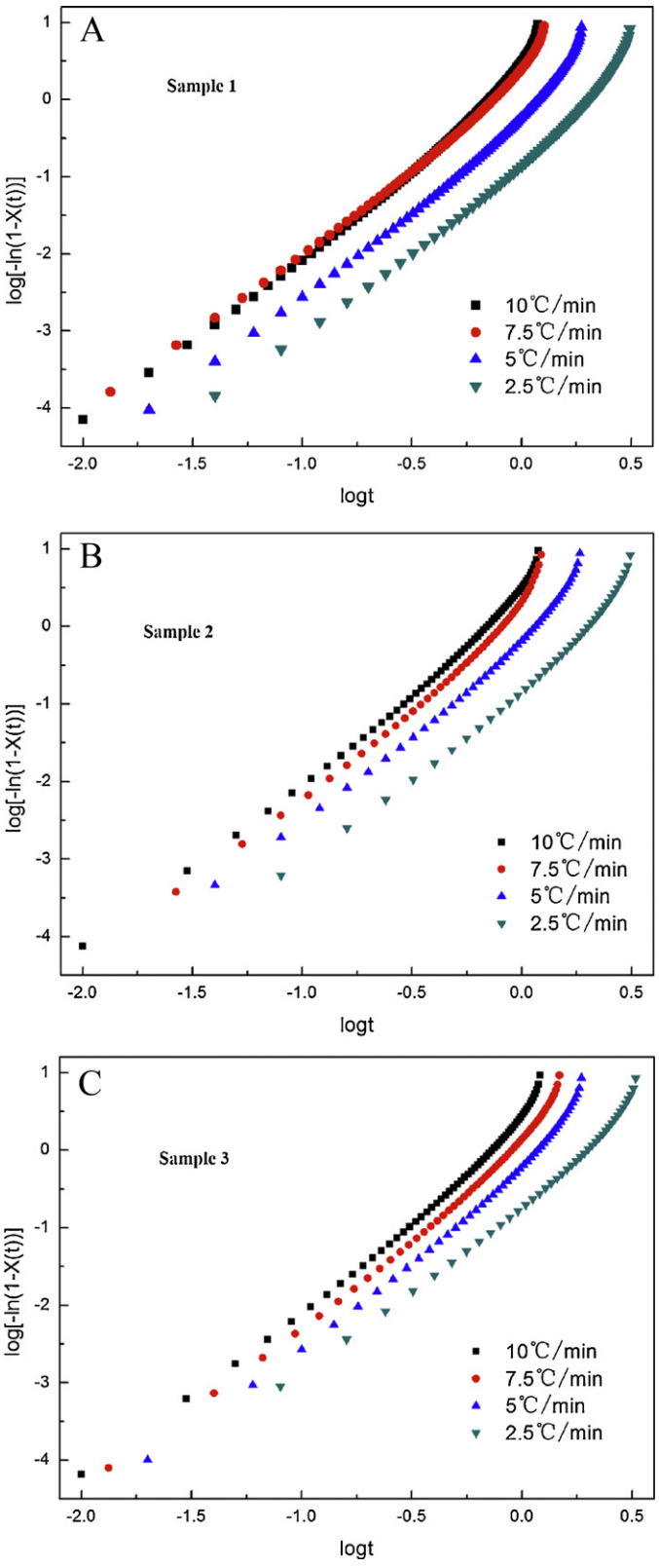

Fig. 4. The plot of $\log[-\ln(1-X)] \sim \log t$: (A) Sample **1**, (B) Sample **2**, and (C) Sample **3**.

Table 4
Jeziorny parameters for samples **1**, **2** and **3** at various cooling rates.

Sample no.	R (°C/min)	K	K_c	n_1[a]	n_2[b]
1	2.5	0.0921	0.3852	2.035	3.084
	5	0.3262	0.7993	2.016	2.951
	7.5	0.9705	0.9960	2.083	3.158
	10	0.8235	0.9808	2.008	3.214
2	2.5	0.0929	0.3866	2.037	3.033
	5	0.3198	0.7961	2.026	3.169
	7.5	0.5834	0.9307	2.031	3.164
	10	0.8926	0.9887	1.983	3.210
3	2.5	0.1433	0.4597	2.032	3.057
	5	0.2780	0.7741	2.019	3.071
	7.5	0.4859	0.9083	2.022	3.162
	10	0.7641	0.9735	2.008	2.940

[a] n_1 is the Avrami constant at the first stage.
[b] n_2 is the Avrami constant at the second stage.

the Ozawa exponent, which is dependent on spherulite growth model and nucleation mechanism. Ozawa equation can be rearranged into double logarithmic form:

$$\log[-\ln(1-X)] = \log K(T) - m\log R \tag{7}$$

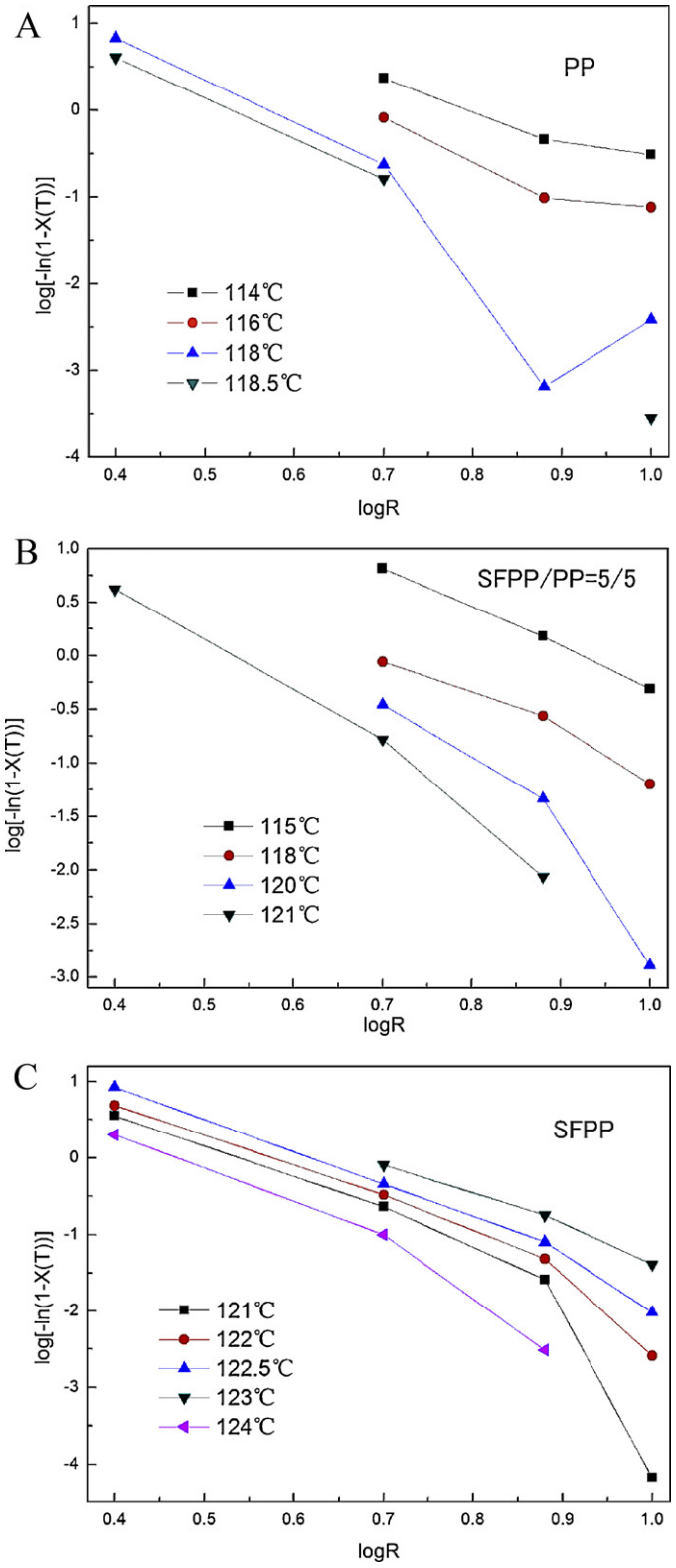

Fig. 5. Ozawa plots of $\log[-\ln(1-X)] \sim \log R$: (A) Sample **1**, (B) Sample **2**, and (C) Sample **3**.

Table 5
The Mo parameters for samples **1**, **2** and **3** at various relative crystallinities.

Sample no.	X (%)					
		10%	30%	50%	70%	90%
1	$F(T)$	0.3566	0.5922	0.7135	0.8096	0.9158
	α	1.1384	1.1730	1.1965	1.2216	1.2615
2	$F(T)$	0.3271	0.5852	0.7133	0.8129	0.9186
	α	1.2526	1.2559	1.2657	1.2790	1.2990
3	$F(T)$	0.2504	0.5784	0.7316	0.8453	0.9626
	α	1.5039	1.4368	1.4095	1.3967	1.3937

According to the Ozawa analysis, if the relative crystallinities at different cooling rates at a given temperature are chosen, the plot of $\log[-\ln(1-X)] \sim \log R$ should give a series of parallel lines, then K and m can be calculated from the intercept and slope, respectively.

However, the plots of $\log[-\ln(1-X)]$ versus $\log R$ for all the samples are non-linear and fail to give the Ozawa exponent m and rate constant K (Fig. 5). Thus, Ozawa model does not provide a satisfactory description for the nonisothermal crystallization process of SFPP/PP blend.

2.2.3. Mo analysis

Mo et al. [10] developed a new form of kinetic equation by combining Avrami and Ozawa equation for the nonisothermal crystallization. The Avrami equation relates the relative crystallinity X with the crystallization time t, and the Ozawa equation relates the relative crystallinity X with the rate of cooling R, therefore, the combination of these two models derives a new kinetic equation for the nonisothermal crystallization:

$$\log R = \log F(T) - \alpha \log t \tag{8}$$

where $F(T) = [K(T)/K]^{1/m}$ refers to the required cooling rate when the measured system reaches a given crystallinity at the unit crystallization time; α is the ratio of the Avrami exponent (n) divided by the Ozawa exponent (m). According to Eq. (8), plotting $\log R$ against $\log t$ is carried out, and fortunately, straight lines are obtained for all the samples, indicating Mo model shows reasonably good agreement for the SFPP/PP blend (Fig. 6).

Values of $F(T)$ and α calculated from the intercept and slope are listed in Table 5. Apparently, $F(T)$ has a trend to increase with the relative crystallinity X, meaning that choosing higher cooling rates is useful for enhancing relative crystallinity. And at the same relative crystallinity, $F(T)$ is slightly increased for samples **2** and **3** by comparison with sample **1**, demonstrates that the addition of SFPP can decrease the crystallization rate. Meanwhile, all the α values are bigger than 1, suggesting the Avrami exponent is bigger than the Ozawa exponent in these cases [11].

2.2.4. Activation energy of crystallization

The effective activation energy of crystallization is an important parameter for the crystallization behavior. ΔE is usually calculated by Kissinger equation, as follows:

$$\frac{d[\ln(R/T_c^2)]}{d(1/T_c)} = -\frac{\Delta E}{R_p} \tag{9}$$

where R is the crystallization cooling rate, T_c is the peak crystalline temperature, and R_p represents the universal gas constant ($R = 8.3145$ J/mol/K). Accordingly, in the light of the results in Table 2, the plot of $\ln(R/T_c^2) \sim 1/T_c$ is drawn, as shown in Fig. 7, a straight line is obtained. The activation energies for samples **1**, **2** and **3** calculated from the slopes are listed in Table 6.

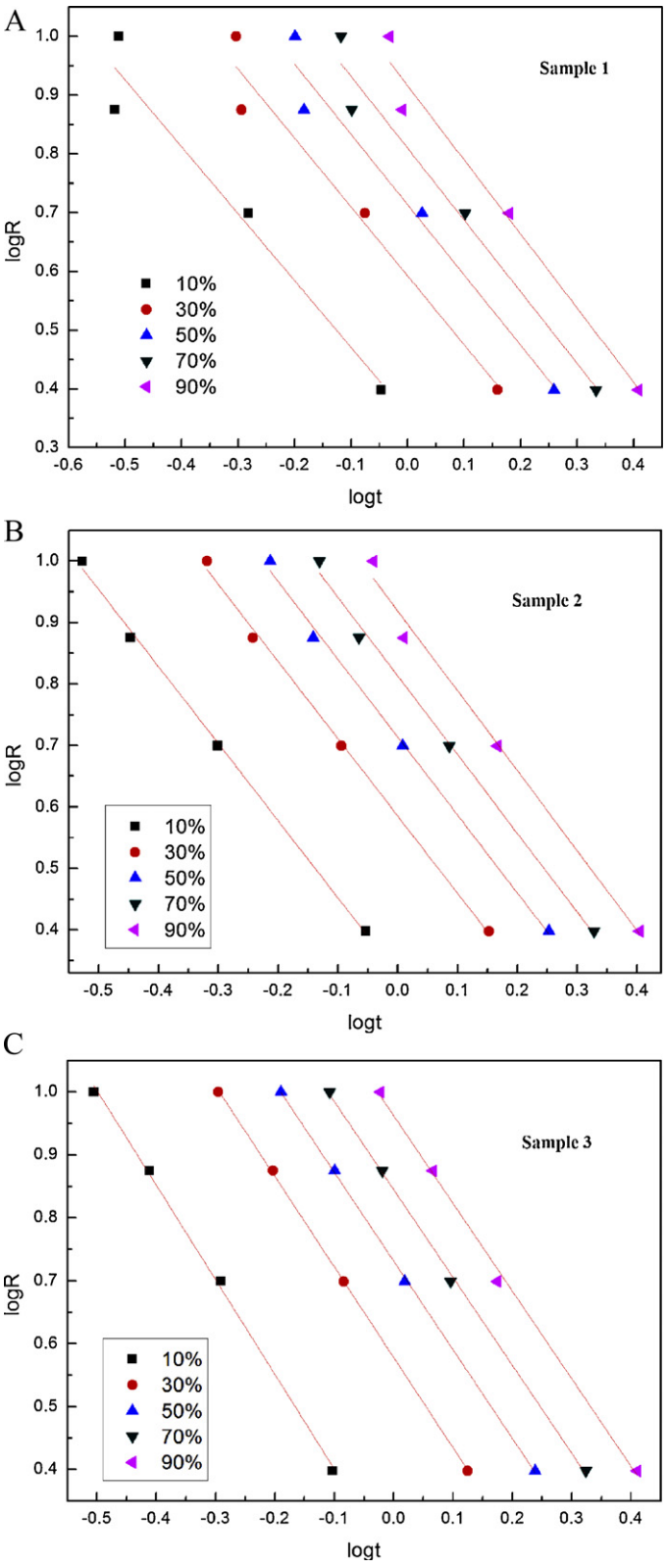

Fig. 6. The plot of log $R \sim \log t$ for the samples **1**, **2** and **3**: (A) Sample **1**, (B) Sample **2**, and (C) Sample **3**.

As observed from Table 6, ΔE value is −19.27 kJ/mol for sample **1**, while −19.55 kJ/mol for sample **2**, and −21.28 kJ/mol for sample **3**, which indicates that the addition of fluorine into PP was not beneficial to its crystallization.

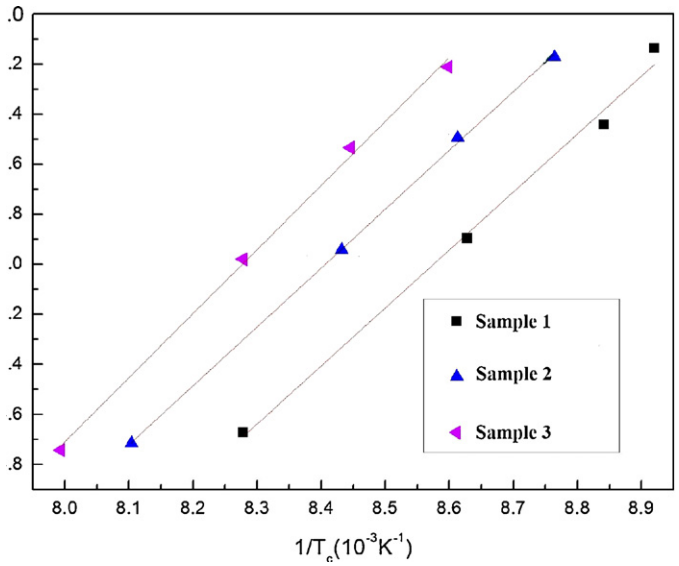

Fig. 7. The plot of $\ln(R/T_c^2) \sim 1/T_c$ for samples **1**, **2** and **3**.

Table 6
The ΔE values for samples **1**, **2** and **3**.

Sample no.	ΔE (kJ/mol)
1	−19.27
2	−19.55
3	−21.28

3. Conclusion

The nonisothermal crystallization behavior of SFPP/PP blend was investigated by DSC technique. DSC diagram SFPP/PP blend shows that the compatibility of the fluorinated PP molecules with the PP matrix is good. A comparison of crystallization parameters indicates T_0, T_c and ΔE are increased, whereas ΔH_c are decreased with the incorporation of fluorine to PP. Nonisothermal crystallization kinetic studies using macrokinetic models such as Jeziorny, Ozawa and Mo method conclude that Mo equation can supply a reasonable description for the nonisothermal crystallization kinetic behavior of SFPP/PP blend.

4. Experimental

Unless otherwise mentioned, reagents were purchased from commercial sources and used as received. Polypropylene (T30s) was purchased from Kunlun Petroleum & Chemical Corporation. Antioxidant 1010 was bought from Ciba Chemicals. 10% F_2 mixing with N_2 (volume percentage) was acquired from Shanghai Science Bio-Pharmaceutical Co. Ltd. High purity N_2 (99.99%) was bought from Shanghai Pujiang Special Gas. The steel fluorinating reactor was made in our lab. The blending was operated on Haake Rheomix 600P. The EDS analysis was measured on Falion type energy dispersive spectrometer.

4.1. The preparation of surface fluorinated polypropylene particles

Polypropylene particle (100 g, medium radius: 2 mm) was washed with distilled water, dried at 100 °C for 2 h and added to a fluorinating reactor. The reactor was evacuated and filled with N_2 alternatively for three times. Diluted 3% F_2/N_2 mixed gas was introduced into the reactor and maintained gas pressure in the reactor at 0.12 MPa for 24 h. Then N_2 was blown for 1 h to drive off

residual F_2 and HF gas from the reactor to a gas-absorbing vessel with 1 M NaOH aqueous solution. The reactor was evacuated and filled in N_2 for three times. Surface fluorinated polypropylene particle was dried at 100 °C for 2 h and stored in a drier for the use in the following experiments.

The EDS analysis showed the surface fluorine content of the SFPP particle was 9.36 at%.

4.2. The preparation of SFPP/PP blend

The mixture of PP, SFPP and antioxidant 1010 was added into a Haake torque rheometer, and mixed at 180 °C with 60 rpm for 15 min. Pressed the mixture in a press vulcanizer to form 1 mm board: the mixture was posed in the mold, preheated at 180 °C for 7 min, pressed at 180 °C for 5 min and at 117 °C for 2 min, finally in a cold press for 7 min. After that they were exposed in the air for 24 h for the following test.

4.3. Differential scanning calorimetry (DSC)

Nonisothermal crystallization kinetics was carried out by using a NETZSCH DSC 200 PC, the temperature was calibrated with indium. Very small cut portions from the specimen of about 300–500 μm size, weight 7–9 mg, were used in the study to ensure better heat transfer from the DSC pan to the sample. In the nonisothermal crystallization process, the samples were heated at a selected constant rates (in the range from 2.5 to 10 °C/min) from room temperature up to 200 °C, held there for 2 min to eliminate small residual nuclei that might be acted as seed crystals, and then the melts was cooled to crystallize at the selected constant cooling rates to 80 °C. All operations were performed under a nitrogen purge.

Acknowledgment

We thank for the financial support by Guizhou Wengfu (Group) Co. Ltd.

Appendix A. Supplementary data

Supplementary data associated with this article can be found, in the online version, at http://dx.doi.org/10.1016/j.jfluchem.2012.09.011.

References

[1] G. Houghan, P.E. Cassidy, K. Johns, T. Davidsion, Fluoropolymers, Kluwer Academic, Plenum Publishers, New York, 1999.
[2] (a) A.P. Kharitonov, Journal of Fluorine Chemistry 103 (2000) 123–127;
(b) A.P. Kharitonov, Journal of Fluorine Chemistry 126 (2005) 251–263;
(c) A.P. Kharitonov, Progress in Organic Coatings 61 (2008) 192–204.
[3] (a) T. Kasai, T. Aya, H. Ohara, Journal of Applied Polymer Science 86 (2002) 684–691;
(b) E. Uhse, D. Hass, M. Schoenherr, A. Zimmerling, DD280772.;
(c) H. Heinrich, S. Manfred, DE3910770.;
(d) T. Sekine, M. Mutsushiro, JP63218064.;
(e) M. Eschwey, R. van Bonn, D.C. Neumann, EP270776.
(f) A.P. Kharitonov, in: I.V. Gardiner (Ed.), Fluorine Chemistry Research Advances, Nova Science Publishers, Inc., NY, 2007, pp. 35–103;
(g) A.P. Kharitonov, Direct Fluorination of Polymers, Nova Science Publishers Inc., NY, 2008;
(h) A.P. Kharitonov, L.N. Kharitonova, Pure and Applied Chemistry 81 (2009) 451–471;
(i) A.P. Kharitonov, in: J.E. Gray (Ed.), Polystyrene: Properties, Performance and Applications, Nova Science Publishers Inc., NY, 2011, pp. 95–118;
(j) A.P. Kharitonov, G.V. Simbirtseva, V.M. Bouznik, M.G. Chepezubov, M. Dubois, K. Guerin, A. Hamwi, H. Kharbache, F. Masin, Journal of Polymer Science Part A: Polymer Chemistry 49 (2011) 3559–3573.
[4] (a) A.K. Gupta, V.B. Gupta, R.H. Peters, W.G. Harland, J.P. Berry, Journal of Applied Polymer Science 27 (1982) 4669–4686;
(b) A.K. Grupta, S.N. Purwar, Journal of Applied Polymer Science 29 (1984) 1595–1690;
(c) R.Y. Zhang, D.Z. Ma, Polymeric Materials Science and Engineering 7 (1991) 57–60.
[5] H.N. Beck, H.D. Ledbetter, Journal of Applied Polymer Science 9 (1965) 2131–2142.
[6] (a) J.R. Liu, J. Xu, H.C. Dong, Q. Yu, Acta Physicochimica Sinica 28 (2012) 528–535;
(b) X. Liu, A.H. He, K. Du, C.C. Han, Journal of Applied Polymer Science 119 (2011) 162–172;
(c) Z.C. Wang, K.C. Kou, M. Chao, H. Bi, L.K. Yan, Journal of Applied Polymer Science 117 (2010) 1218–1226;
(d) W.J. Lu, X.L. Zhu, Y.M. Zhang, H.P. Wang, C.S. Wang, Y.T. Ye, Journal of Macromolecular Science – Physics 46 (2007) 949–962;
(e) Q. Yuan, S. Awate, R.D.K. Misra, European Polymer Journal 42 (2006) 1994–2003.
[7] (a) M.J. Avrami, Chemical Physics 8 (1940) 212–217;
(b) C.B. Street, Y. Yarovoy, N.J. Wagner, M.S. Vethamuthu, K.D. Hermanson, K.P. Ananthapadmanabhan, Colloids and Surfaces A 406 (2012) 13–23;
(c) E.G. Merino, C. Rodrigues, M.T. Viciosa, C. Melo, J. Sotomayor, M. Dionísio, N.T. Correia, Journal of Physical Chemistry B 115 (2011) 12336–12347;
(d) J.S. Blázquez, C.F. Conde, A. Conde, Journal of Non-Crystalline Solids 357 (2011) 2833–2839;
(e) K. Magnie, B.L. Fox, M.G. Looney, Journal of Polymer Science Part B: Polymer Physics 47 (2009) 1300–1312;
(f) S. Şanlı, A. Durmus, N. Ercan, Journal of Applied Polymer Science 125 (2012) 268–281.
[8] (a) A. Jeziorny, Polymer 19 (1978) 1142–1144;
(b) G. Antoniadis, K.M. Paraskevopoulos, D. Bikiaris, K. Chrissafis, Thermochimica Acta 510 (2010) 103–112;
(c) L.Y. Wang, G. Li, Y.M. Chen, S. Li, Polymer Engineering and Science 52 (2012) 1621–1628;
(d) J. Zhang, S.J. Chen, J. Su, X.M. Shi, J. Jin, X.L. Wang, Z.Z. Xu, Journal of Thermal Analysis and Calorimetry 97 (2009) 959–967.
[9] (a) T. Ozawa, Polymer 12 (1971) 150–158;
(b) F. Bertini, M. Canetti, G. Ricci, European Polymer Journal 45 (2009) 923–931;
(c) Z.M. Chen, Y. Liu, C.G. Yao, G.S. Yang, Polymer Testing 31 (2012) 685–696;
(d) E. Chiavaro, L. Cerretani, M. Paciulli, S. Vecchio, Journal of Thermal Analysis and Calorimetry 108 (2012) 799–806;
(e) R.M.R. Wellen, E. Canedo, M.S. Rabello, Journal of Materials Research 26 (2011) 1107–1115;
(f) C. Zhang, Y. Huang, Y. Liu, S. Wang, X. Zhang, Pigment and Resin Technology 38 (2009) 79–90;
(g) H.Y. Bai, Y. Zhang, Y.X. Zhang, X.F. Zhang, W. Zhou, Journal of Applied Polymer Science 101 (2006) 1295–1308.
[10] (a) T.X. Liu, Z.S. Mo, S.G. Wang, H.F. Zhang, Polymer Engineering and Science 37 (1997) 568–575;
(b) Z.M. Chen, C.G. Yao, G.S. Yang, Polymer Testing 31 (2012) 393–403.
[11] G.P. Balamurugan, S.N. Maiti, Journal of Applied Polymer Science 107 (2008) 2414–2435.